Supplementary Information for:

Effect of adatom species on structure, stability, and work function of adatom-α-borophene nanocomposites

Jing He,[a] Bing Zheng,*[a] Ying Xie,[a] Yin-yin Qian,[a] Jiao Zhang,[a] Ke Wang,[a] Lin Yang,[bc] and Hai-tao Yu*[a]

[a] *Key Laboratory of Functional Inorganic Material Chemistry (Ministry of Education) and School of Chemistry and Materials Science, Heilongjiang University, Harbin 150080, P. R. China. E-mail: zhengbing0106@163.com, yuhaitao@hlju.edu.cn*

[b] *National Key Laboratory of Science and Technology on Advanced Composites in Special Environments, Center for Composite Materials and Structures, Harbin Institute of Technology, Harbin 150080, P. R. China*

[c] *School of Aerospace, Mechanical and Mechatronic Engineering, The University of Sydney, Sydney, NSW 2006, Australia*

Contents of the Supporting Information:

Fig. S8 Optimized BBP structures containing one magnesium atom.

Fig. S9 Optimized BBP structures containing one calcium atom.

Fig. S10 Optimized BBP structures containing one strontium atom.

Fig. S11 Optimized BBP structures containing one barium atom.

Fig. S12 Optimized BBP structures containing one fluorine atom.

Fig. S13 Optimized BBP structures containing one chlorine atom.

Fig. S14 Optimized BBP structures containing one bromine atom.

Fig. S15 Optimized BBP structures containing one iodine atom.

Fig. S16 Constant-T simulation of alkali metal/BBP using the Nosé-Hoover chain thermostat, with a time step of 1.5 fs, target temperature of 300 K, and nose Q ratio of 2.0. (a)–(e) show the potential energies of Li/BBP, Na/BBP, K/BBP, Rb/BBP, and Cs/BBP at each time step of the simulation within 3 ps, respectively.

Fig. S17 Constant-T simulation of alkaline earth metal/BBP using the Nosé-Hoover chain thermostat, with a time step of 1.5 fs, target temperature of 300 K, and nose Q ratio of 2.0. (a)–(e) show the potential energies of Be/BBP, Mg/BBP, Ca/BBP, Sr/BBP, and Ba/BBP at each time step of the simulation within 3 ps, respectively.

Fig. S18 Constant-T simulation of halogen/BBP using the Nosé-Hoover chain thermostat, with a time step of 1.5 fs, target temperature of 300 K, and nose Q ratio of 2.0. (a)–(d) show the potential energies of F/BBP, Cl/BBP, Br/BBP, and I/BBP at each time step of the simulation within 3 ps, respectively.

Fig. S19 Hirshfeld charges of adatom (M), NB, and RB in (a) alkali metal/BBP and (b) alkaline earth metal/BBP as a function of ionization potential (IP). (c) Hirshfeld charges of M, NB, and the sum of RB and SNB (RB+SNB) in halogen/BBP as a function of electronegativity (χ).

Fig. S20 Electron density differences for (a) F/BBP, (b) Cl/BBP, (c) Br/BBP, (d) I/BBP, and (e) diagram of M and two boron atoms used to determine the indicated slice aMb.

Fig. S21 (a) PDOSs of the s, p, and d orbitals of alkaline earth metal atoms before adsorption. (b) PDOSs of the s, p, and d orbitals of alkaline earth metal atoms after adsorption. (c) PDOSs of the s, p, and d orbitals of boron atoms of alkaline earth metal/BBP before and after adsorption.

Fig. S22 (a) PDOSs of the s, p, and d orbitals of halogen atoms before adsorption. (b) PDOSs of the s, p and, d orbitals of halogen atoms after adsorption. (c) PDOSs of the s, p, and d orbitals of boron atoms of halogen/BBP before and after adsorption.

S1 Calculation details

S1.1 Calculating details of induced dipole moment:

The dipole moment p(A) at the surface induced by the adatoms (M) can be defined as

$$p(A) = p(M/BBP) - p(BBP) - p(M) \quad \text{(S1)}$$

where p(M/BBP), p(BBP), and p(M) represent the dipole moments of M/BBP, the BBP substrate, and the adatoms, respectively.

S1.2 Calculating details of dipole moment:

Dipole moment vector of M/BBP ($\mu_{M/BBP}$) can be obtained by the following formula

$$\sum_{a=1}^{n} q_{M/BBP,a} r_{M/BBP,a} \tag{S2}$$

where $q_{M/BBP,a}$ refers to the partial charge of atom a in M/BBP, while $r_{M/BBP,a}$ represents the position vector of atom a in M/BBP.

S2 Tables

Table S1 Work functions of graphene, silicene, BN-sheet, and borophene before and after atom adsorption in previous studies. ϕ (eV) and ϕ_A (eV) are the work functions of a 2D material before and after adsorption, respectively. $\Delta\phi$ (eV) refers to the variation of the work function by adsorption.

Adatom	Material	ϕ	ϕ_A	$\Delta\phi$	Functional
Li	graphene	4.26	2.72	−1.54	PBE[1]
Na	graphene	4.26	2.21	−2.05	PBE[1]
K	graphene	4.26	1.49	−2.77	PBE[1]
Ca	graphene	4.26	3.18	−1.08	PBE[1]
Al	graphene	4.26	3.08	−1.18	PBE[1]
Ga	graphene	4.26	2.66	−1.60	PBE[1]
In	graphene	4.26	2.34	−1.92	PBE[1]
Sn	graphene	4.26	3.81	−0.45	PBE[1]
Ti	graphene	4.26	3.16	−1.10	PBE[1]
Fe	graphene	4.26	3.24	−1.02	PBE[1]
Pd	graphene	4.26	3.61	−0.65	PBE[1]
Au	graphene	4.26	4.88	0.62	PBE[1]
Li	graphene	4.38	2.57 ~ 3.53	−1.81 ~ −0.85	PBE[2]
Na	graphene	4.38	2.45 ~ 3.34	−1.93 ~ −1.04	PBE[2]
K	graphene	4.38	2.23 ~ 3.22	−2.15 ~ −1.16	PBE[2]
Rb	graphene	4.38	2.20 ~ 3.15	−2.18 ~ −1.23	PBE[2]
Cs	graphene	4.38	2.06 ~ 3.04	−2.32 ~ −1.34	PBE[2]
Ca	graphene	4.38	2.91 ~ 3.46	−1.47 ~ −0.92	PBE[2]
Sr	graphene	4.38	2.84 ~ 3.38	−1.54 ~ −0.10	PBE[2]
Al	graphene	4.38	3.06 ~ 3.62	−1.81 ~ −0.85	PBE[2]
Ti	graphene	4.38	3.10 ~ 3.73	−1.28 ~ −0.65	PBE[2]
N	graphene	4.38	4.70 ~ 5.20	0.32 ~ 0.82	PBE[3]
P	graphene	4.38	4.60 ~ 4.80	0.22 ~ 0.42	PBE[3]
As	graphene	4.38	4.50 ~ 4.78	0.12 ~ 0.42	PBE[3]
O	graphene	4.38	4.80 ~ 4.90	0.42 ~ 0.52	PBE[3]
S	graphene	4.38	4.50 ~ 4.75	0.12 ~ 0.32	PBE[3]
Se	graphene	4.38	4.50 ~ 4.74	0.12 ~ 0.42	PBE[3]
F	graphene	4.38	4.80 ~ 5.30	0.42 ~ 0.92	PBE[3]
Cl	graphene	4.38	5.20 ~ 5.76	0.82 ~ 1.42	PBE[3]

To be continued.

Adatom	Material	ϕ	ϕ_A	$\Delta\phi$	Functional
Br	graphene	4.38	5.00 ~ 5.71	0.62 ~ 1.32	PBE[3]
I	graphene	4.38	5.00 ~ 5.70	0.62 ~ 1.32	PBE[3]
F	silicene	4.59	5.85	1.26	PBE[4]
Cl	silicene	4.59	5.35	0.76	PBE[4]
Br	silicene	4.59	5.17	0.58	PBE[4]
I	silicene	4.59	4.91	0.32	PBE[4]
K	BN-sheet	2.85	0.98	−1.87	PWGGA[5]
Na	BN-sheet	2.85	1.76	−1.09	PWGGA[5]
Li	BN-sheet	2.85	1.93	−0.92	PWGGA[5]
Ca	BN-sheet	2.85	2.15	−0.70	PWGGA[5]
Mg	BN-sheet	2.85	2.67	−0.18	PWGGA[5]
Be	BN-sheet	2.85	3.19	0.34	PWGGA[5]
Li	α-borophene	4.16	3.67 ~ 2.31	−0.49 ~ −1.85	PW91[6]
Li	2-layer α-borophene	4.65	4.46 ~ 1.96	−0.19 ~ −2.69	PBE[7]
Li	α_1-borophene	4.19	3.61 ~ 1.58	−0.58 ~ −2.61	PW91[8]
Na	α_1-borophene	4.19	3.38 ~ 1.17	−0.81 ~ −3.02	PW91[8]
K	α_1-borophene	4.19	3.07 ~ 0.68	−1.12 ~ −3.51	PW91[8]
Cs	α-borophene	4.16	3.05 ~ 0.11	−1.11 ~ −4.04	PW91[9]
F	α-borophene	4.14	5.36 ~ 7.78	1.22 ~ 3.64	PBE[10]
H	δ_6-borophene	5.31	5.88	0.57	HSE06[11]
Li	germanene	–	3.86	–	PBE[12]
Na	germanene	–	3.59	–	PBE[12]
K	germanene	–	3.27	–	PBE[12]
Be	germanene	–	4.59	–	PBE[12]
Mg	germanene	–	4.39	–	PBE[12]
Ca	germanene	–	3.58	–	PBE[12]
Al	germanene	–	4.37	–	PBE[12]
Ga	germanene	–	4.08	–	PBE[12]
In	germanene	–	3.71	–	PBE[12]
Ti	germanene	–	4.98	–	PBE[12]
V	germanene	–	5.12	–	PBE[12]
Cr	germanene	–	4.84	–	PBE[12]
Fe	germanene	–	4.65	–	PBE[12]
Co	germanene	–	4.75	–	PBE[12]
Ni	germanene	–	4.34	–	PBE[12]
F	2-layer graphene	4.44	5.32	0.79	Exp.[13]
F	4-layer graphene	4.39	4.43 ~ 5.13	0.04 ~ 0.74	Exp.[14]

Table S2 Migration pathways of M adatoms and corresponding energy barriers (eV) for different adatoms on BBP or other 2D materials in this study and previous studies. H1, F1, B1, and T1 are the equilibrium adsorption sites on the corresponding 2D material. H2, F2, and T2 are the other adsorption sites.

Structure	Migration pathway	Energy barrier	Ref
Li/BBP	H1 → H2	0.28	this work
Na/BBP	H1 → H2	0.28	this work
K/BBP	H1 → H2	0.16	this work
Rb/BBP	H1 → H2	0.10	this work
Cs/BBP	H1 → H2	0.07	this work
Be/BBP	H1 → H2	–[a]	this work
Mg/BBP	H1 → H2	1.90	this work
Ca/BBP	H1 → H2	0.01	this work
Sr/BBP	H1 → H2	0.14	this work
Ba/BBP	F1 → H2	0.00	this work
F/BBP	F1 → F2	1.96	this work
Cl/BBP	F1 → F2	1.30	this work
Br/BBP	F1 → F2	1.02	this work
I/BBP	F1 → F2	0.04	this work
Li/α-borophene	H1 → H2	0.21	Ref. 6
Na^+/δ_6-borophene	B1 → F2	0.22	Ref. 15
Na/graphene	B1 → H2	0.10	Ref. 1
K/graphene	B1 → H2	0.10	Ref. 1
Cs/α-borophene	H1 → H2	0.43	Ref. 9
Be/BN-sheet	B1 → H2	<1	Ref. 5
Ca/graphene	T1 → H2	0.12	Ref. 16
Sr/BN-sheet	B1 → H2	<1	Ref. 5
Ba/BN-sheet	B1 → H2	<1	Ref. 5
F/δ_6-borophene	T1 → T2	1.26	Ref. 17

[a] unavailable data.

Table S3 Average M–B bond lengths (Å) and average bond angles ($\angle B_mMB_o$, degree) in M/BBP (M = Li, Na, K, Rb, Cs, Be, Mg, Ca, Sr, Ba, F, Cl, Br, and I) before and after NVT-molecular dynamics (NVT-MD) simulations (3 ps). B_m and B_o are two o-position boron atoms in a hexagonal hole nearest to the adatom in BBP, whereas the M in $\angle B_mMB_o$ is M atom decorated on the abovementioned (filled) hexagonal hole.

(a)

	Li/BBP	Na/BBP	K/BBP	Rb/BBP	Cs/BBP	Be/BBP	Mg/BBP
	Average M–B bond length						
Before NVT-MD	2.345	2.752	3.132	3.657	3.508	1.903	2.592
After NVT-MD	2.315	2.719	3.153	3.719	3.524	1.9178	2.550
Variety	−1.28%	−1.19%	0.66%	1.70%	0.46%	0.74%	−1.62%
	Average bond angle ($\angle B_mMB_o$)						
Before NVT-MD	42.021	35.570	31.106	26.554	27.699	53.430	38.294
After NVT-MD	42.690	36.109	31.054	26.711	28.160	53.461	38.794
Variety	1.59%	1.52%	−0.17%	0.59%	1.67%	0.06%	1.31%

(b)

	Ca/BBP	Sr/BBP	Ba/BBP	F/BBP	Cl/BBP	Br/BBP	I/BBP
	Average M–B bond length						
Before NVT-MD	2.718	2.846	3.001	2.858	3.226	3.374	3.575
After NVT-MD	2.735	2.891	3.008	2.851	3.245	3.422	3.645
Variety	0.63%	1.58%	0.22%	1.14%	0.57%	1.43%	1.95%
	Average bond angle ($\angle B_mMB_o$)						
Before NVT-MD	36.401	34.612	32.719	33.674	29.701	28.385	26.759
After NVT-MD	36.244	34.563	33.327	34.134	30.231	28.833	26.988
Variety	−0.43%	−0.14%	1.86%	1.37%	1.78%	1.58%	0.86%

Table S4 Calculated binding energy of M/BBP (E_b, eV), relative torsion energy of the BBP substrate (ΔE_{BBP}, eV), and interaction energy between the adsorbed M atoms and BBP′ in optimized M/BBP models ($E_{M-BBP'}$, eV).

Structure	E_b	ΔE_{BBP}	$E_{M-BBP'}$
Li/BBP	2.321	–0.054	2.375
Na/BBP	1.642	–0.035	1.677
K/BBP	2.063	–0.034	2.098
Rb/BBP	2.238	–0.043	2.282
Cs/BBP	2.660	–0.049	2.709
Be/BBP	2.805	–0.306	3.112
Mg/BBP	0.810	–0.784	1.594
Ca/BBP	2.161	–0.698	2.860
Sr/BBP	2.864	–0.623	3.488
Ba/BBP	4.197	–0.383	4.581
F/BBP	5.327	–0.884	6.212
Cl/BBP	3.300	–0.889	4.190
Br/BBP	2.592	–0.825	3.418
I/BBP	1.959	–0.804	2.763

Table S5 Calculated M–B bond populations of M/BBP systems.

Structure	M–B bond population						
	M–B1	M–B2	M–B3	M–B4	M–B5	M–B6	M–B7
Li/BBP	–0.01	–0.01	–0.01	–0.01	–0.01	–0.01	–
Na/BBP	–0.08	–0.12	–0.13	–0.13	–0.08	–0.12	–
K/BBP	–0.11	–0.11	–0.11	–0.11	–0.11	–0.11	–
Rb/BBP	–0.12	–0.12	–0.12	–0.11	–0.12	–0.11	–
Cs/BBP	–0.12	–0.12	–0.16	–0.12	–0.15	–0.11	–
Be/BBP	0.38	0.07	0.08	0.08	0.38	0.07	–
Mg/BBP	0.06	–0.20	–0.20	–0.20	0.05	–0.20	–0.13
Ca/BBP	–0.23	–0.13	–0.33	–0.33	–0.23	–0.13	0.03
Sr/BBP	0.04	–0.03	–0.11	–0.11	0.04	0.03	0.20
Ba/BBP	0.01	–0.02	–0.02	–0.03	–0.03	0.01	–0.26
F/BBP	0.61	–	–	–	–	–	–
Cl/BBP	0.76	–	–	–	–	–	–
Br/BBP	0.67	–	–	–	–	–	–
I/BBP	0.67	–	–	–	–	–	–

S3 Figures

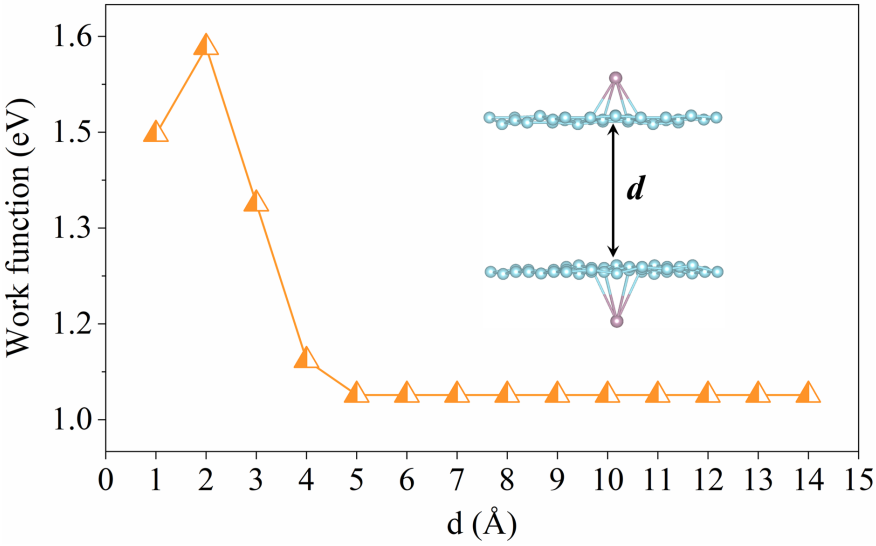

Fig. S1 Work function of Cs/BBP as a function of plane-to-plane (BBP) distance (*d*). Cyan and thistle spheres represent boron and caesium atoms, respectively.

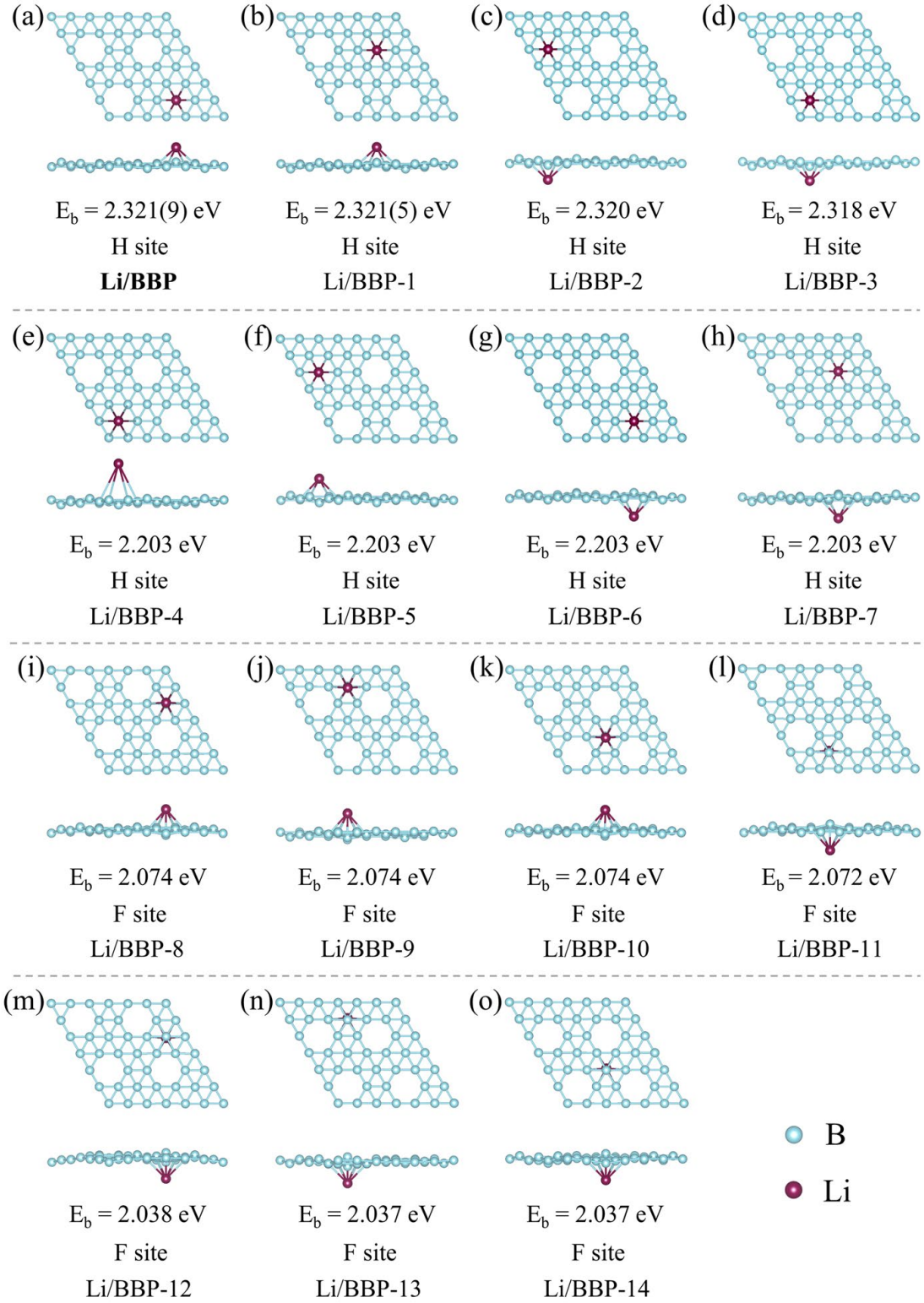

Fig. S2 Optimized BBP structures containing one lithium atom.

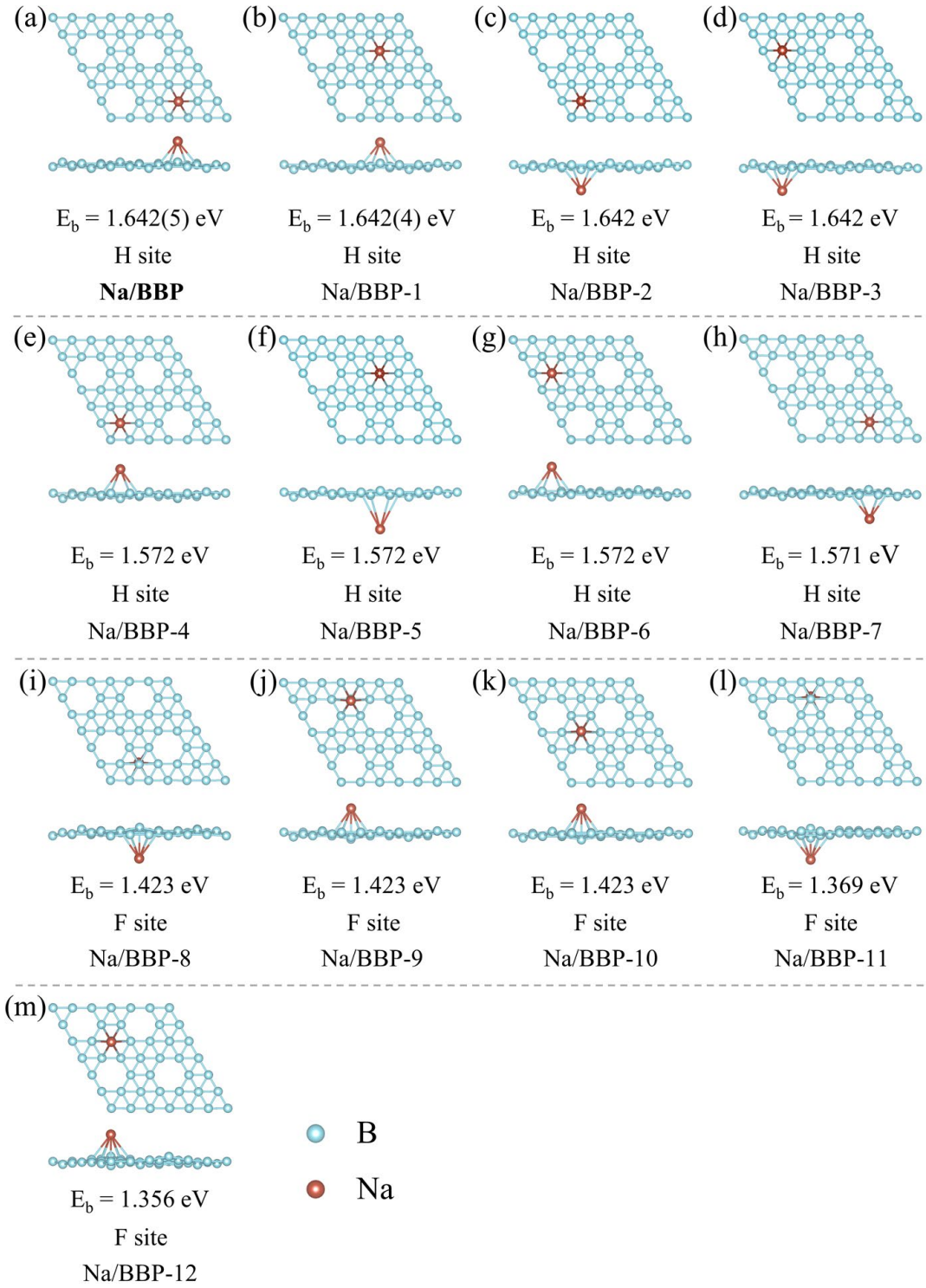

Fig. S3 Optimized BBP structures containing one sodium atom.

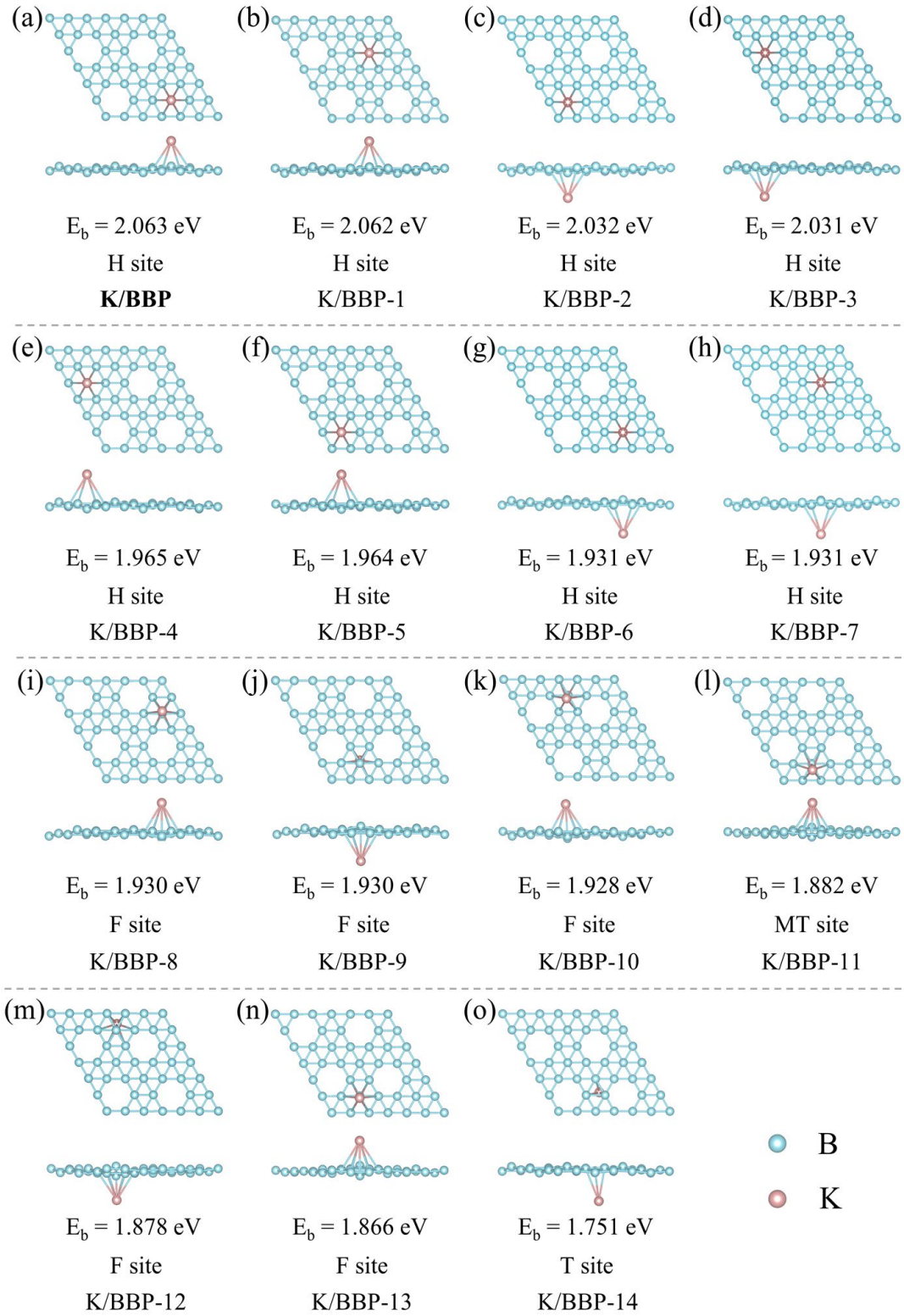

Fig. S4 Optimized BBP structures containing one potassium atom.

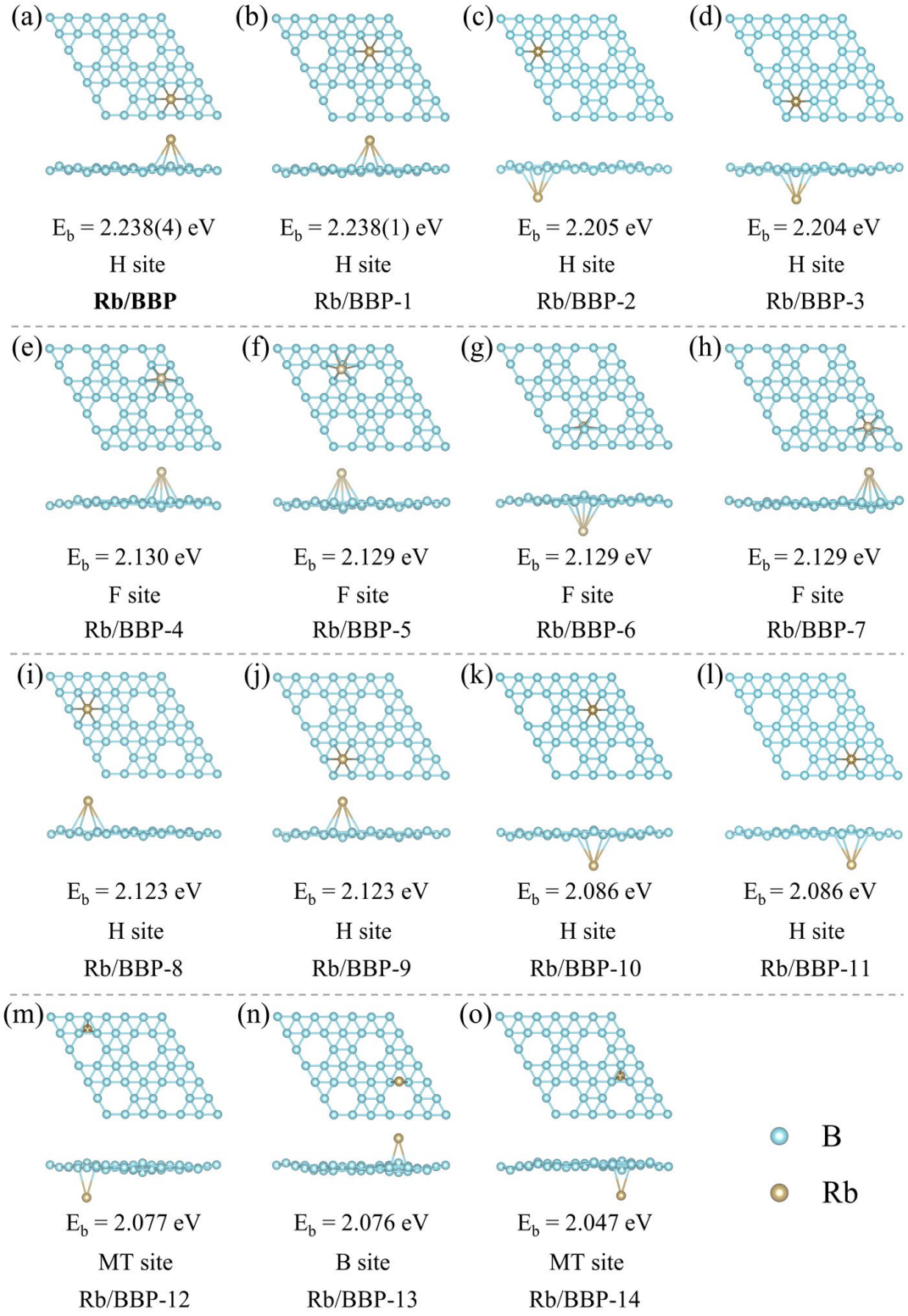

Fig. S5 Optimized BBP structures containing one rubidium atom.

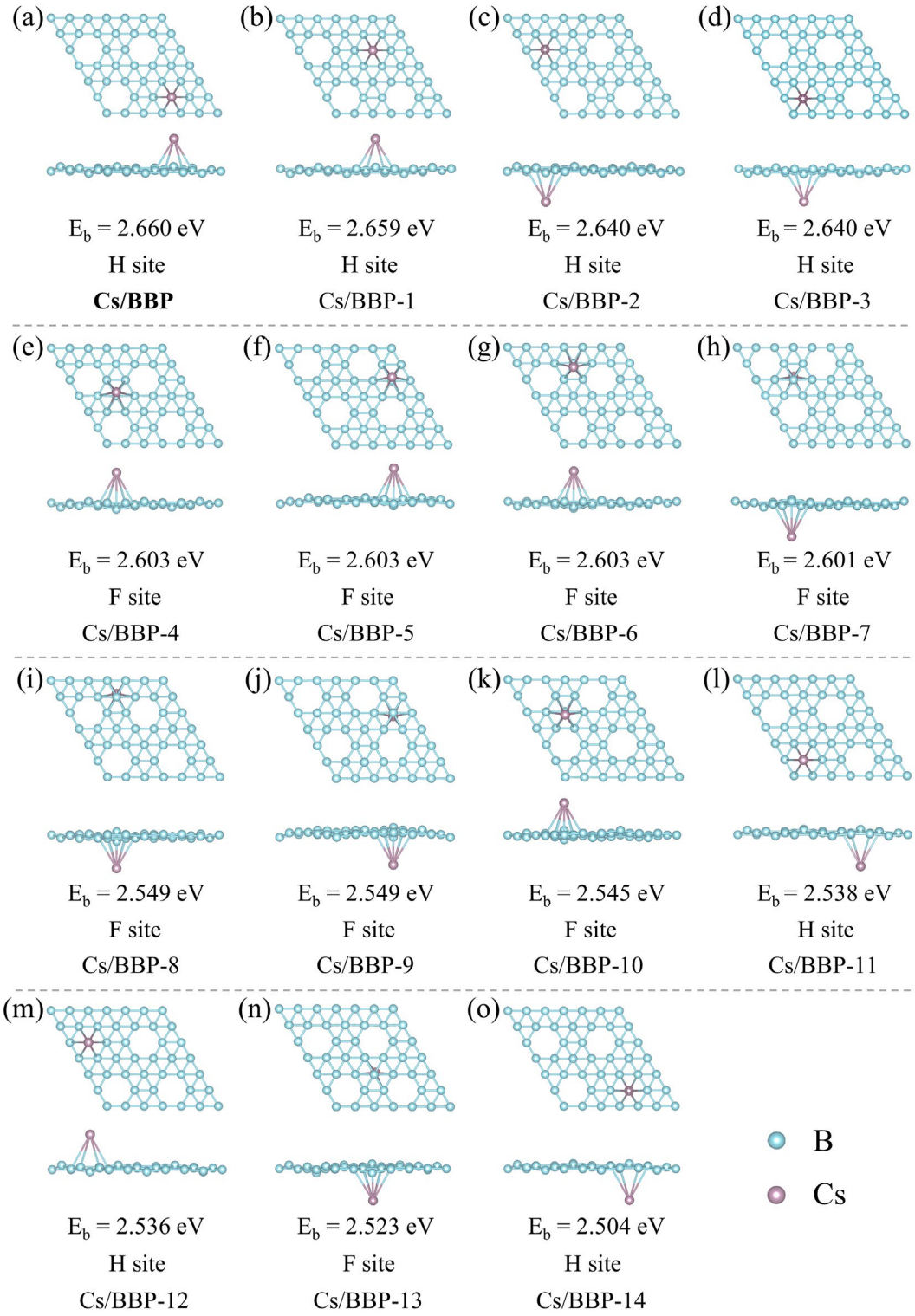

Fig. S6 Optimized BBP structures containing one caesium atom.

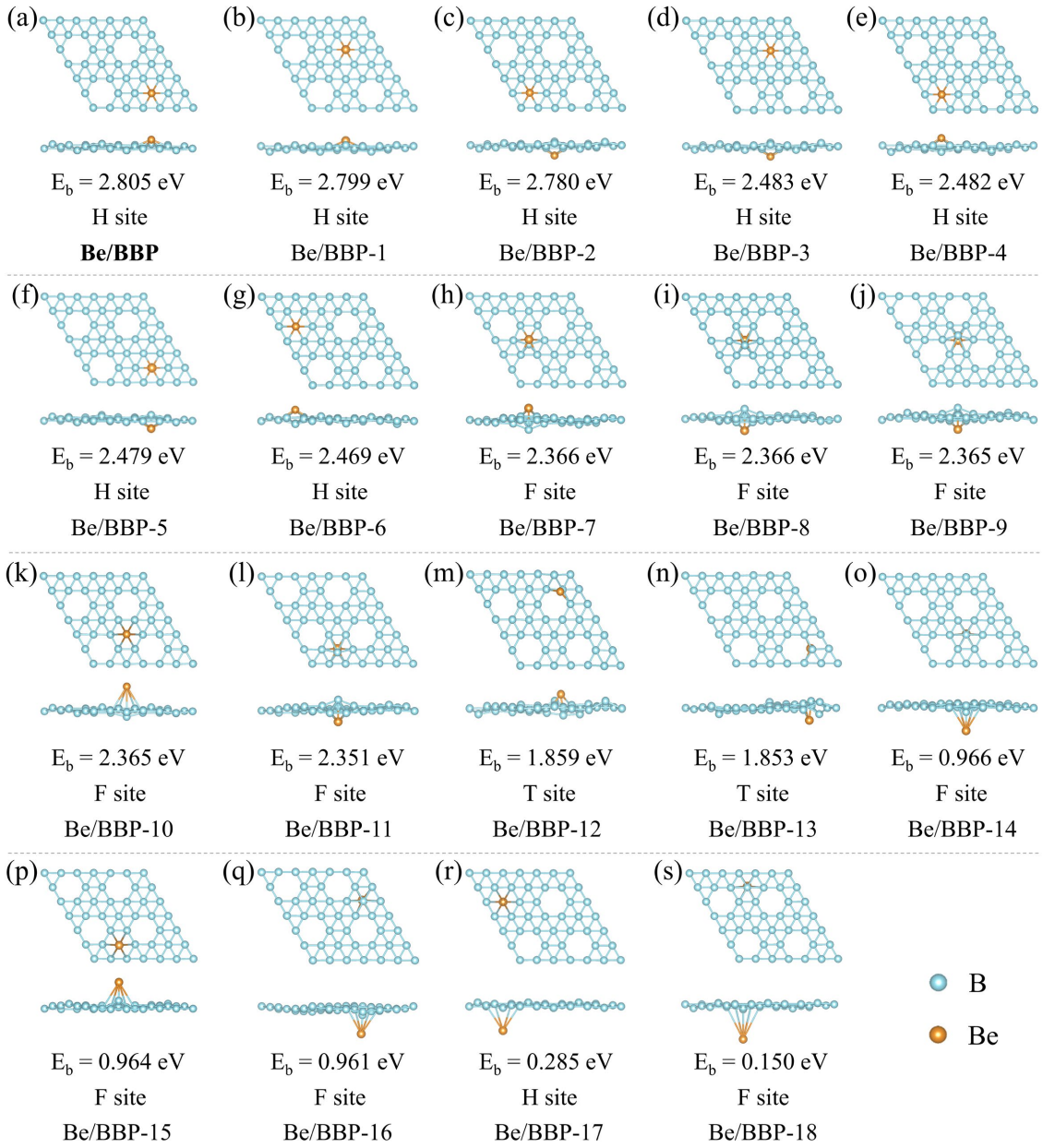

Fig. S7 Optimized BBP structures containing one beryllium atom.

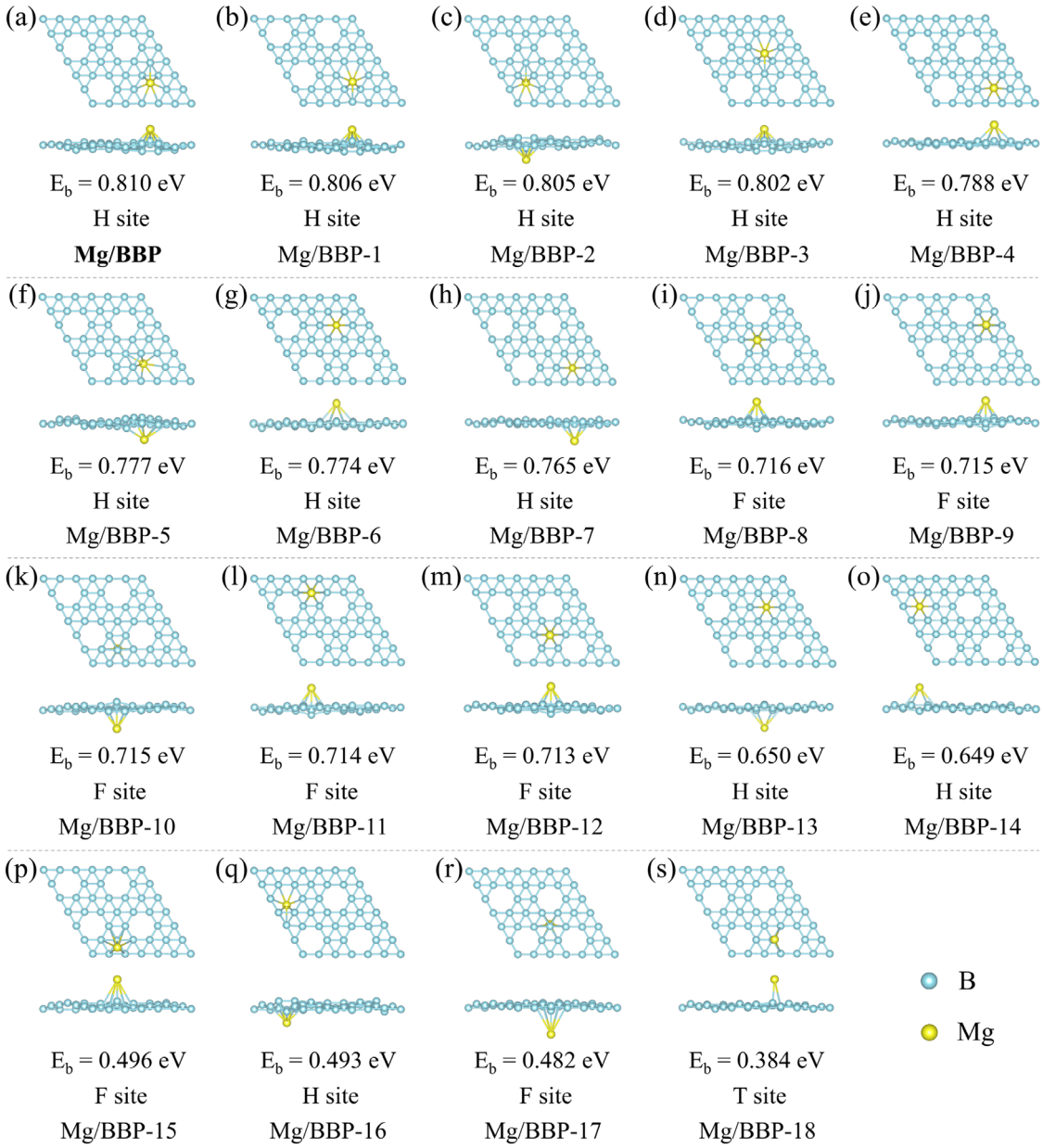

Fig. S8 Optimized BBP structures containing one magnesium atom.

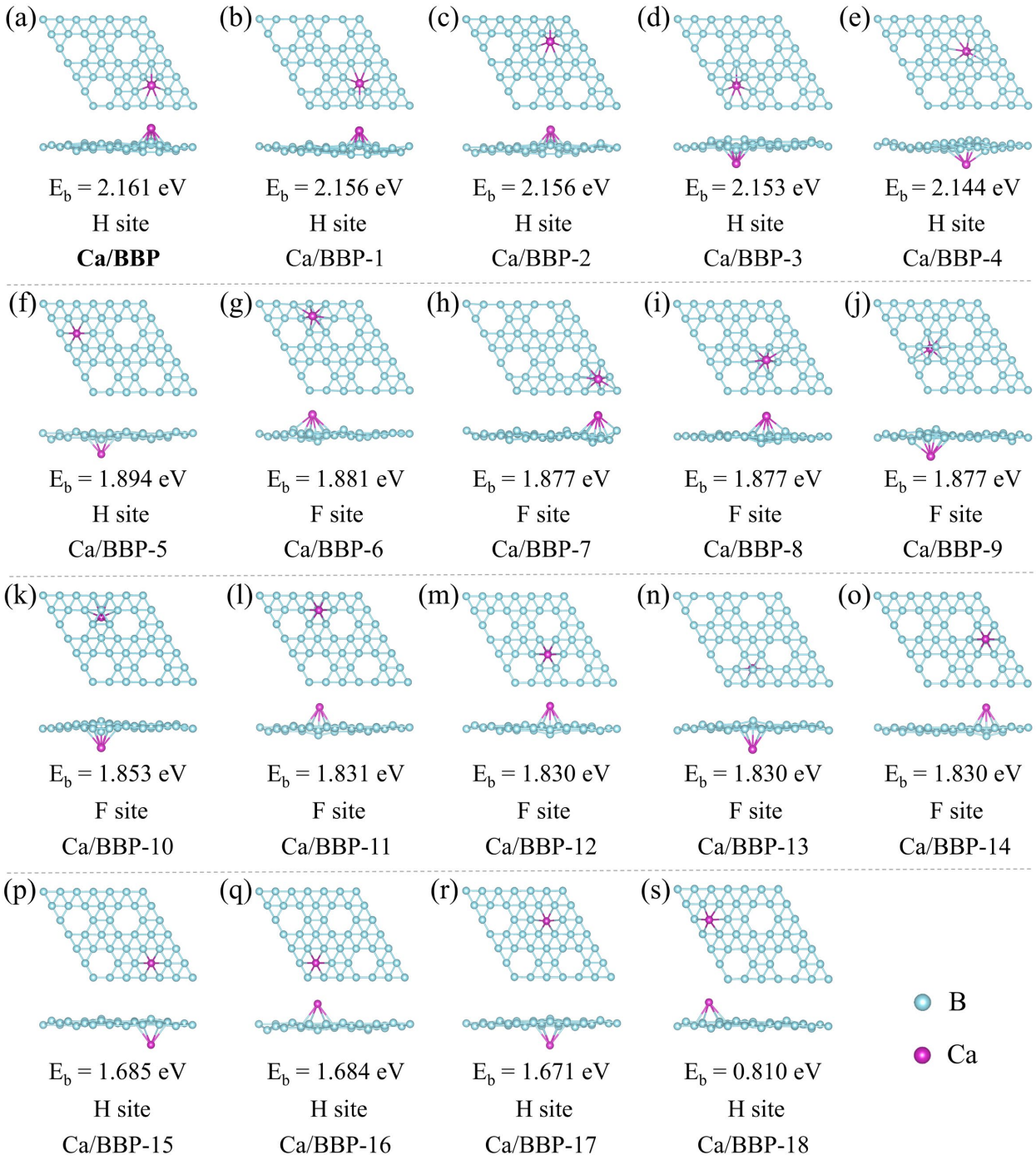

Fig. S9 Optimized BBP structures containing one calcium atom.

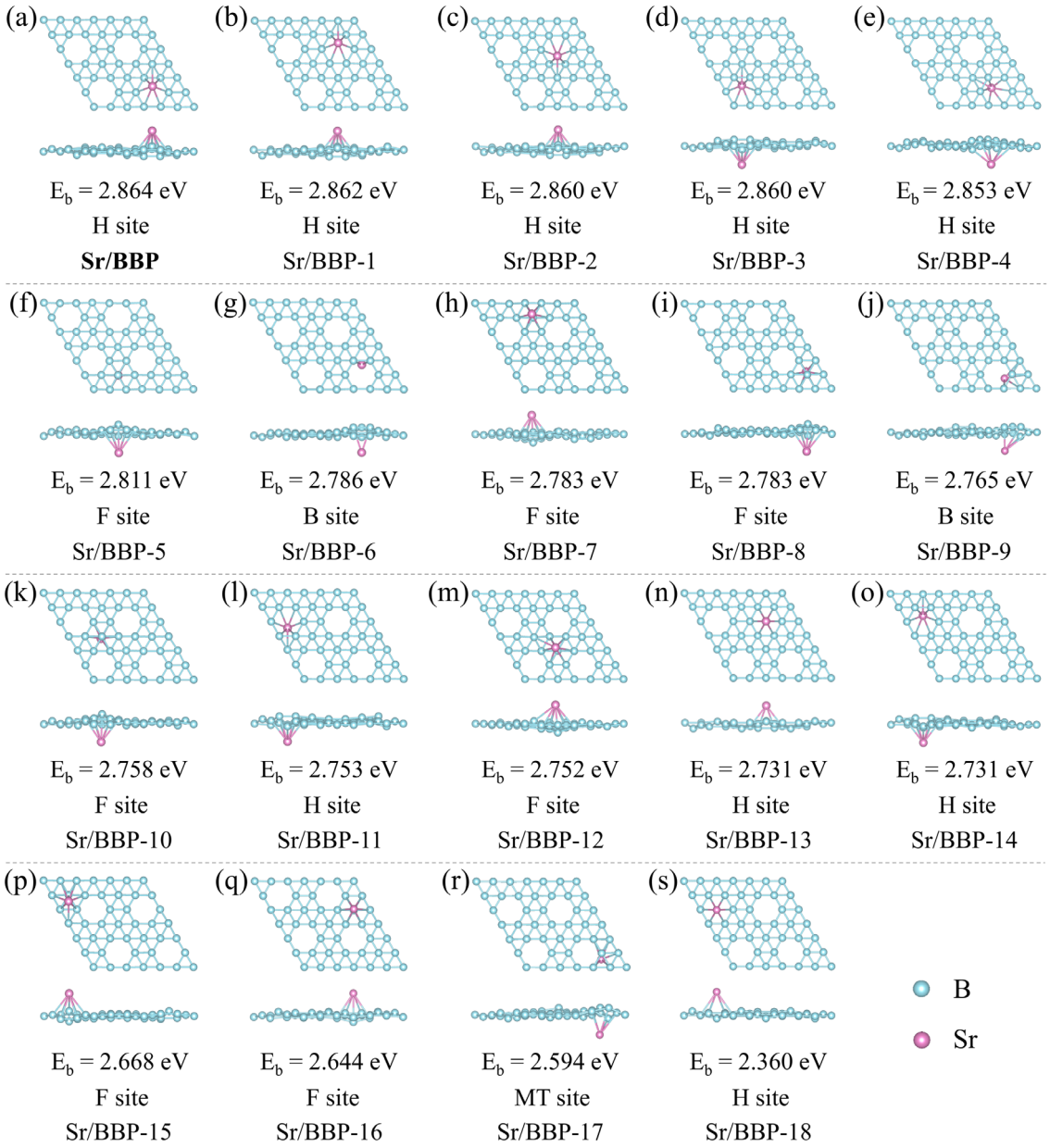

Fig. S10 Optimized BBP structures containing one strontium atom.

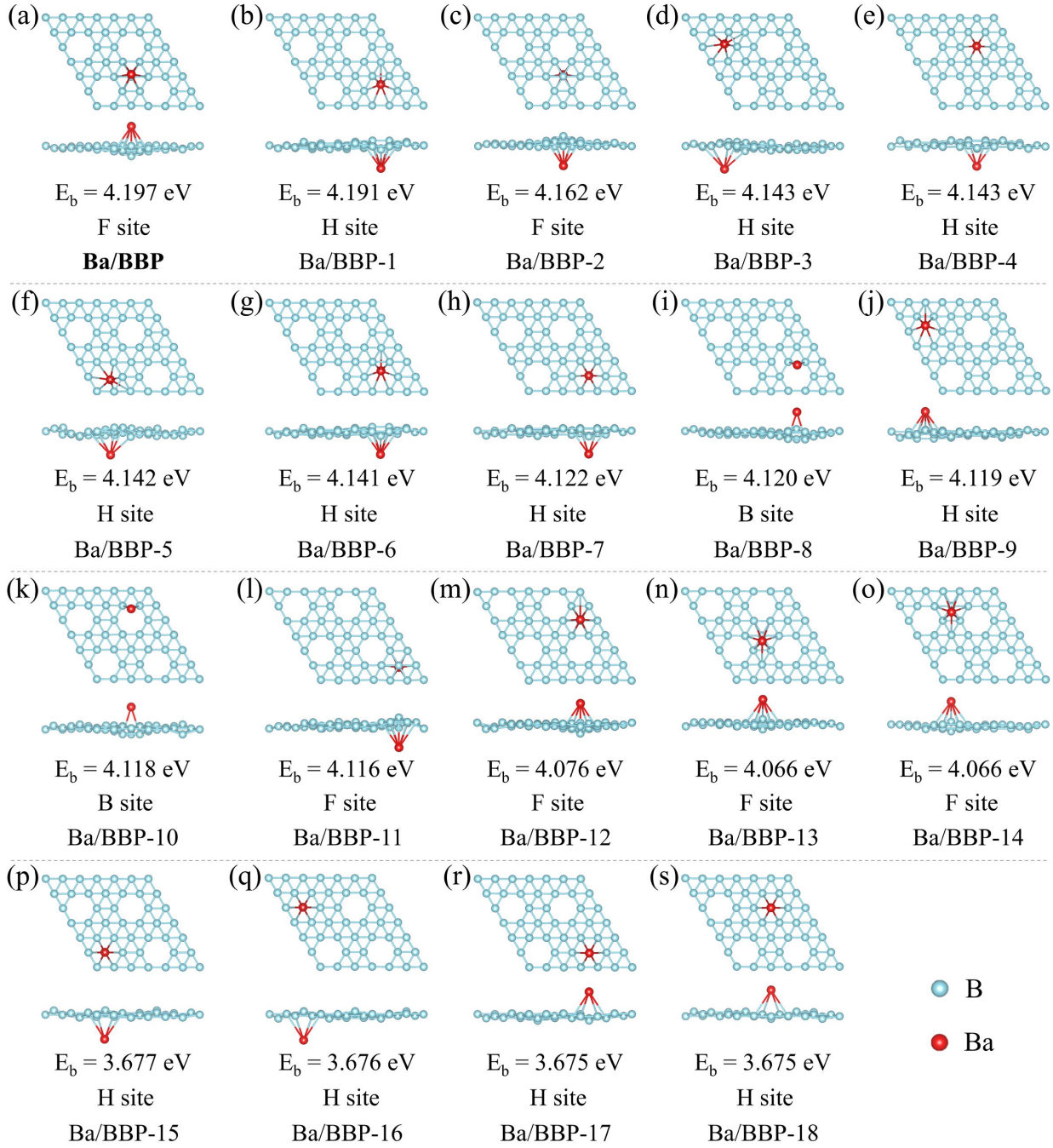

Fig. S11 Optimized BBP structures containing one barium atom.

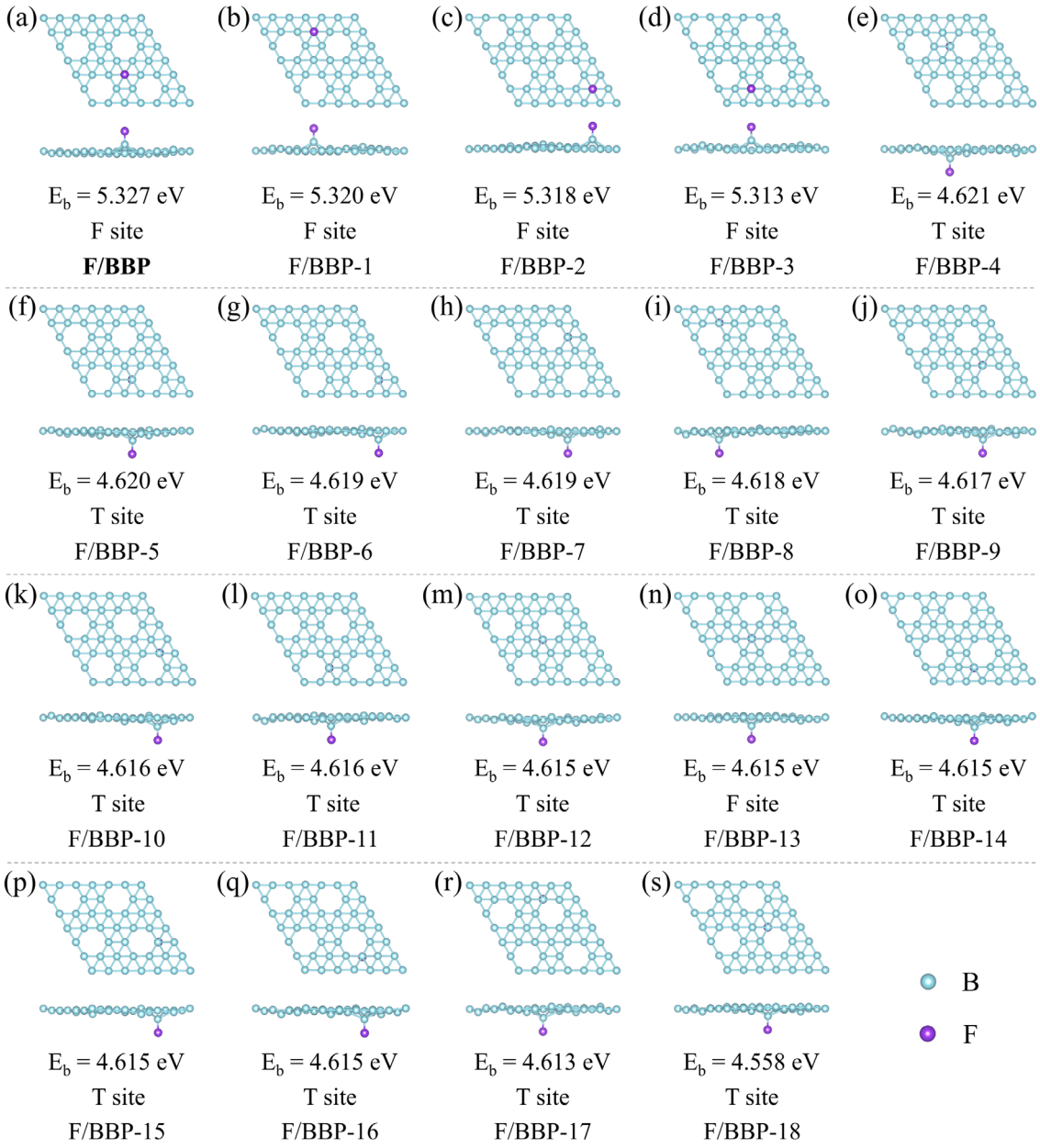

Fig. S12 Optimized BBP structures containing one fluorine atom.

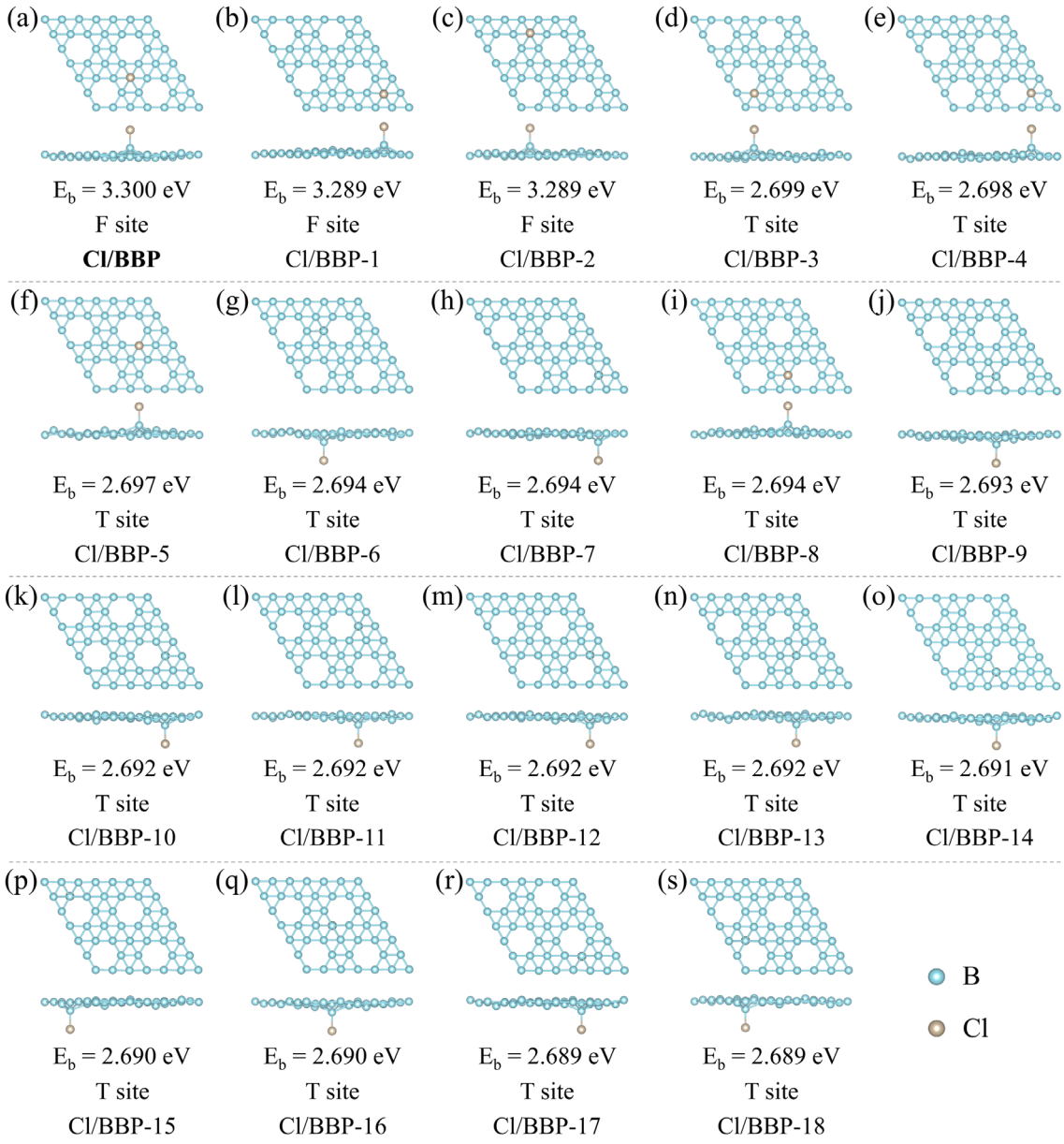

Fig. S13 Optimized BBP structures containing one chlorine atom.

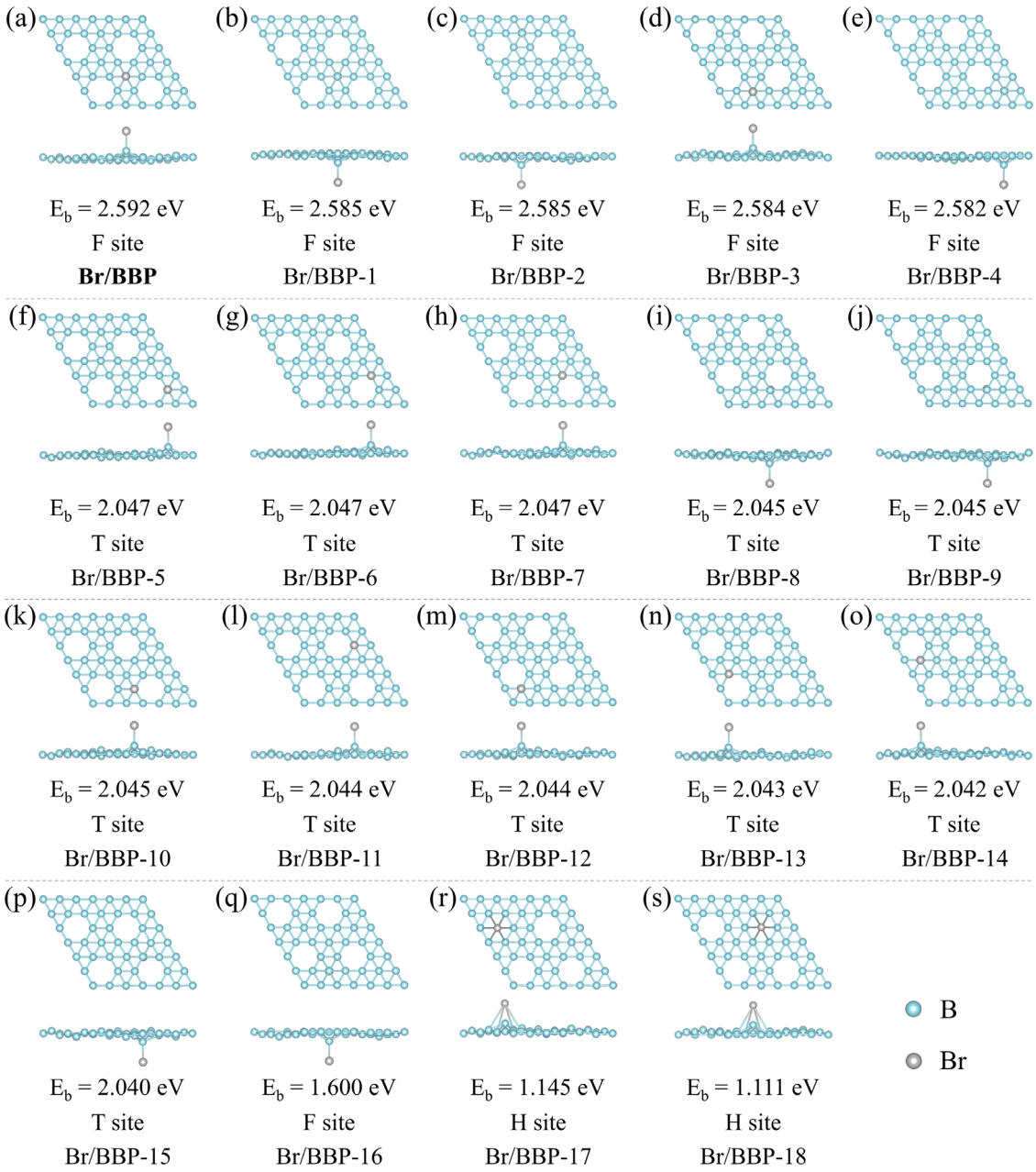

Fig. S14 Optimized BBP structures containing one bromine atom.

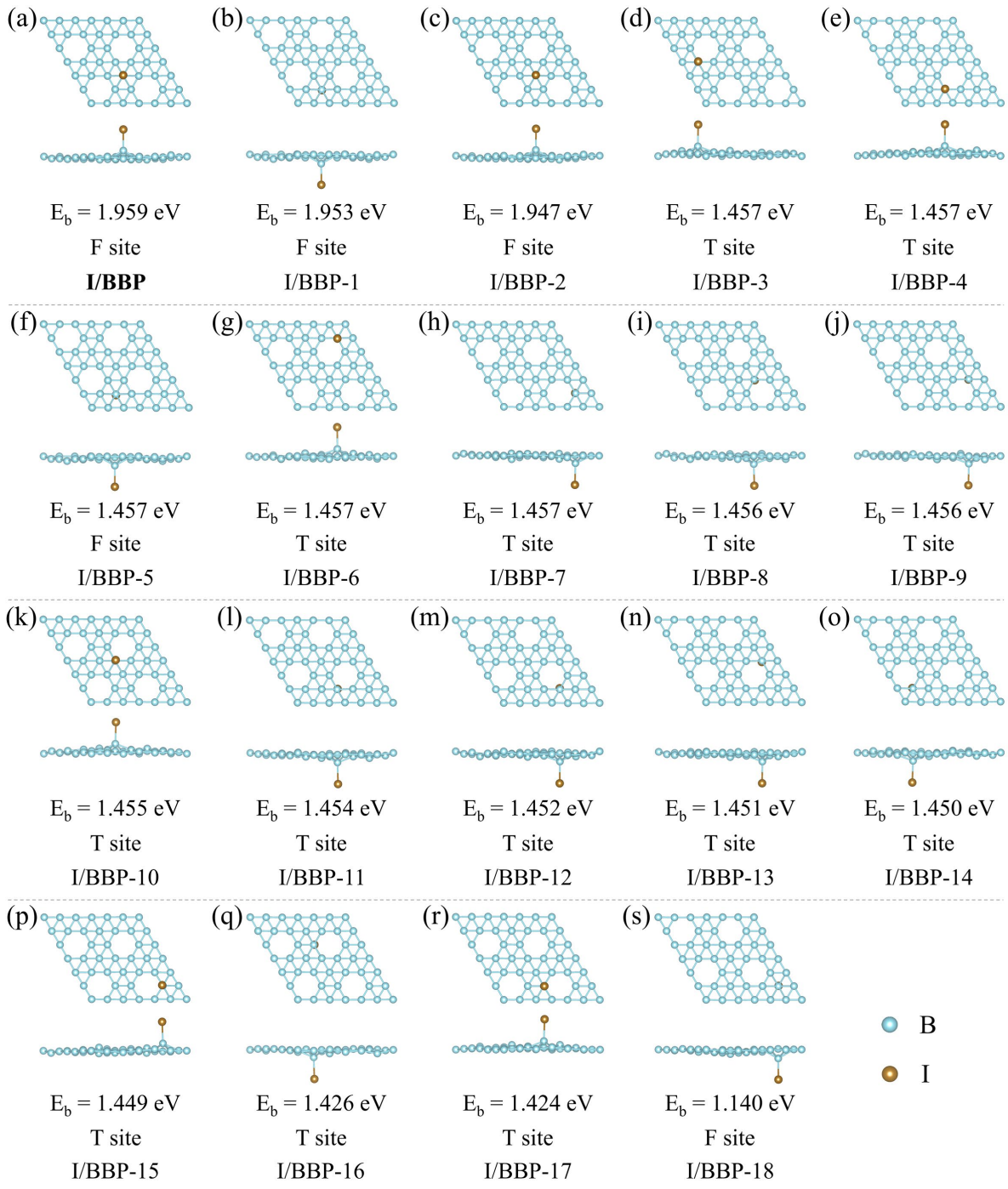

Fig. S15 Optimized BBP structures containing one iodine atom.

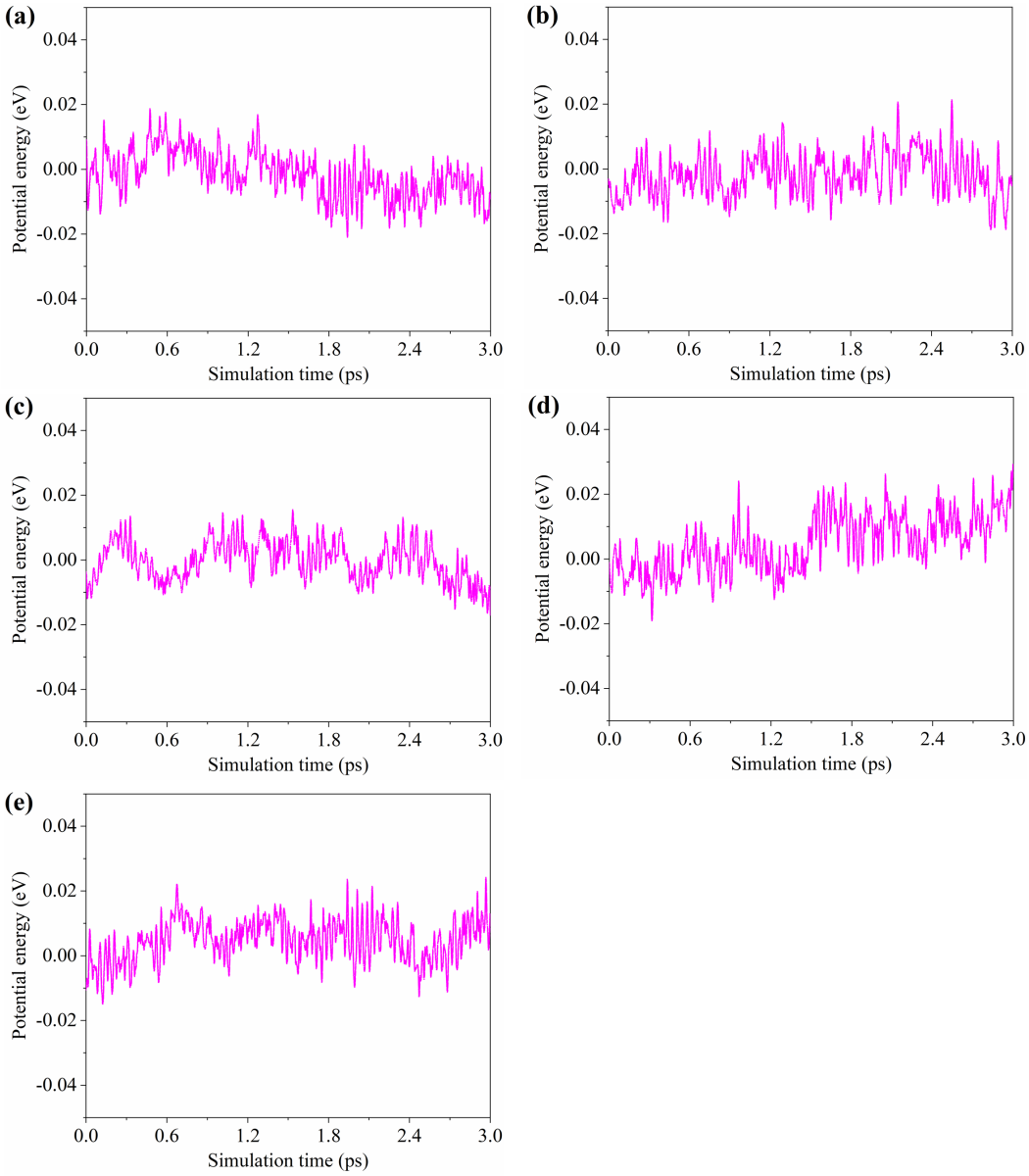

Fig. S16 Constant-T simulation of alkali metal/BBP using the Nosé-Hoover chain thermostat, with a time step of 1.5 fs, target temperature of 300 K, and nose Q ratio of 2.0. (a)–(e) show the potential energies of Li/BBP, Na/BBP, K/BBP, Rb/BBP, and Cs/BBP at each time step of the simulation within 3 ps, respectively.

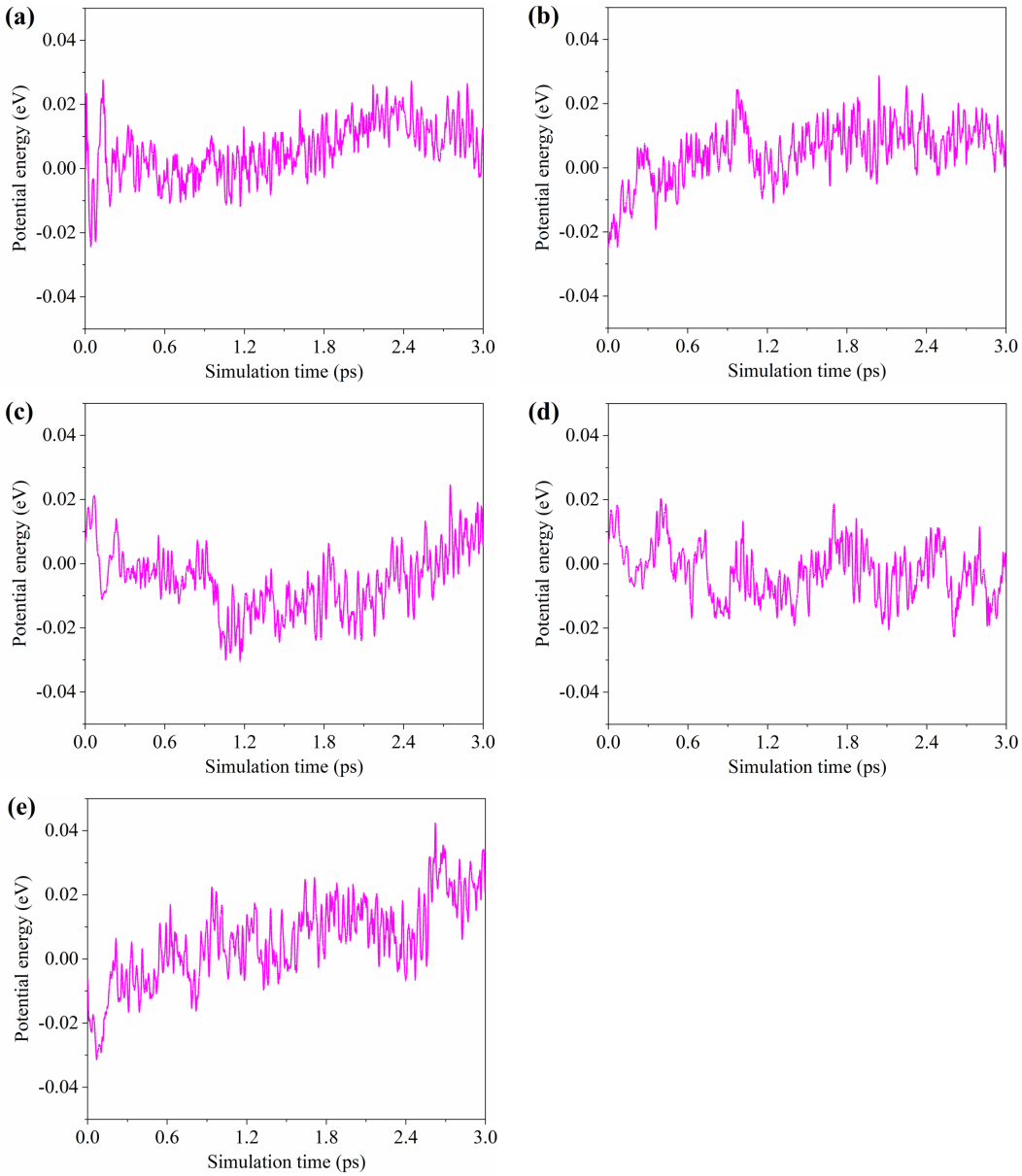

Fig. S17 Constant-T simulation of alkaline earth metal/BBP using the Nosé-Hoover chain thermostat, with a time step of 1.5 fs, target temperature of 300 K, and nose Q ratio of 2.0. (a)–(e) show the potential energies of Be/BBP, Mg/BBP, Ca/BBP, Sr/BBP, and Ba/BBP at each time step of the simulation within 3 ps, respectively.

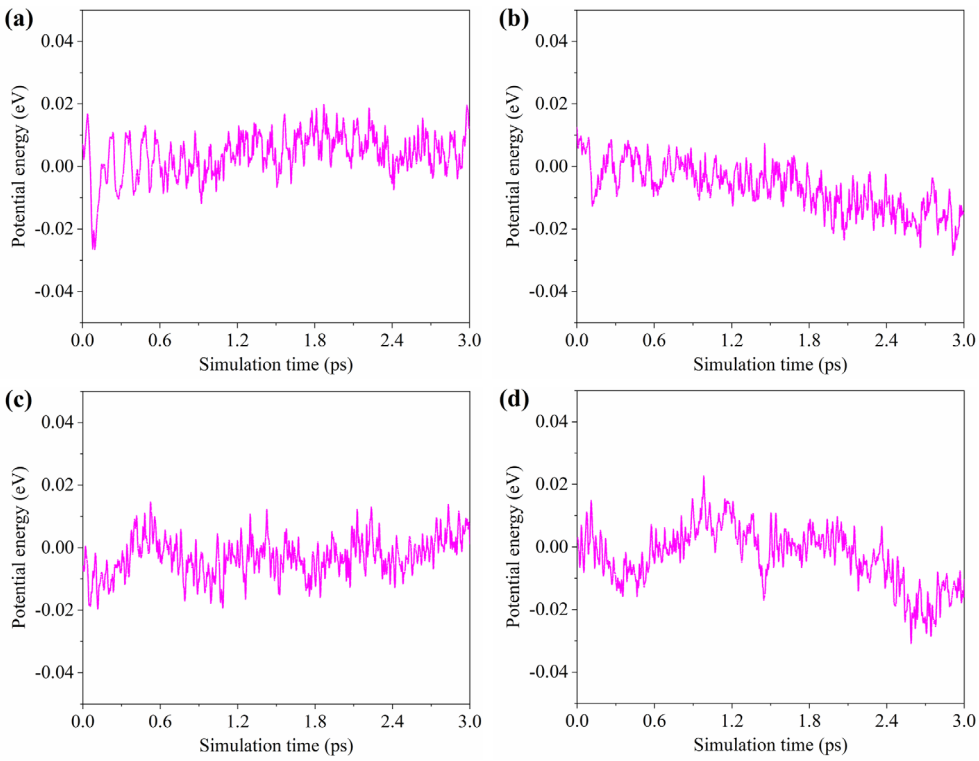

Fig. S18 Constant-T simulation of halogen/BBP using the Nosé-Hoover chain thermostat, with a time step of 1.5 fs, target temperature of 300 K, and nose Q ratio of 2.0. (a)–(d) show the potential energies of F/BBP, Cl/BBP, Br/BBP, and I/BBP at each time step of the simulation within 3 ps, respectively.

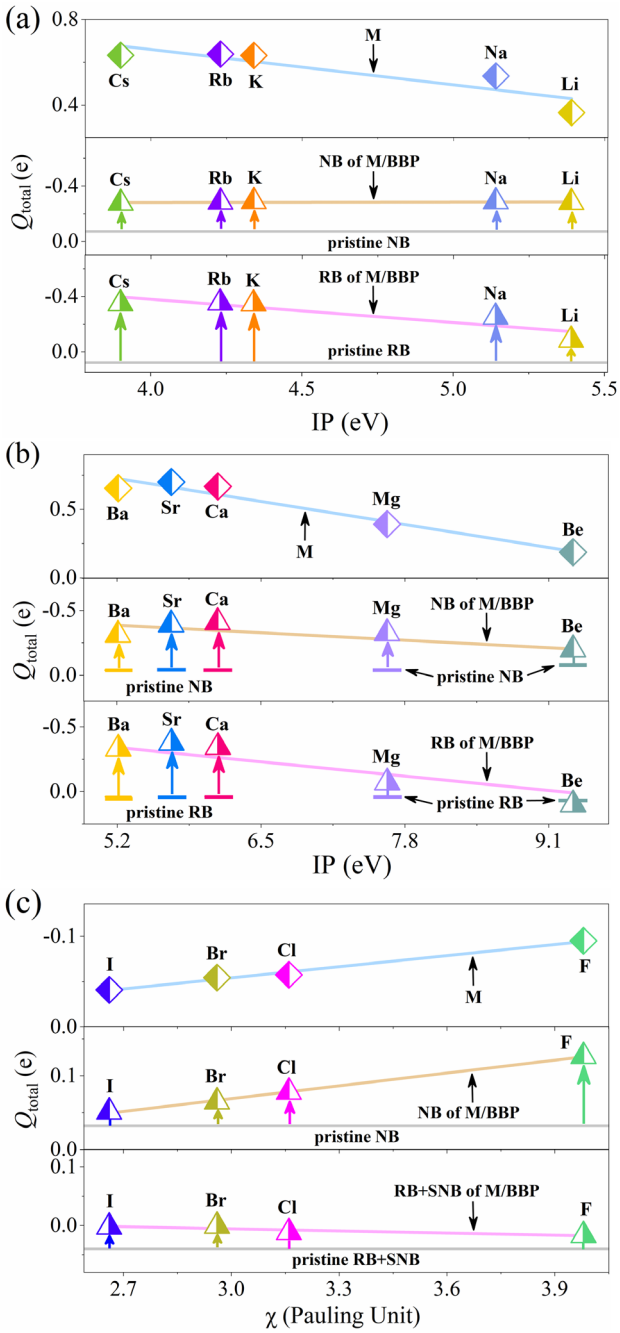

Fig. S19 Hirshfeld charges of adatom (M), NB, and RB in (a) alkali metal/BBP and (b) alkaline earth metal/BBP as a function of ionization potential (IP). (c) Hirshfeld charges of M, NB, and the sum of RB and SNB (RB+SNB) in halogen/BBP as a function of electronegativity (χ).

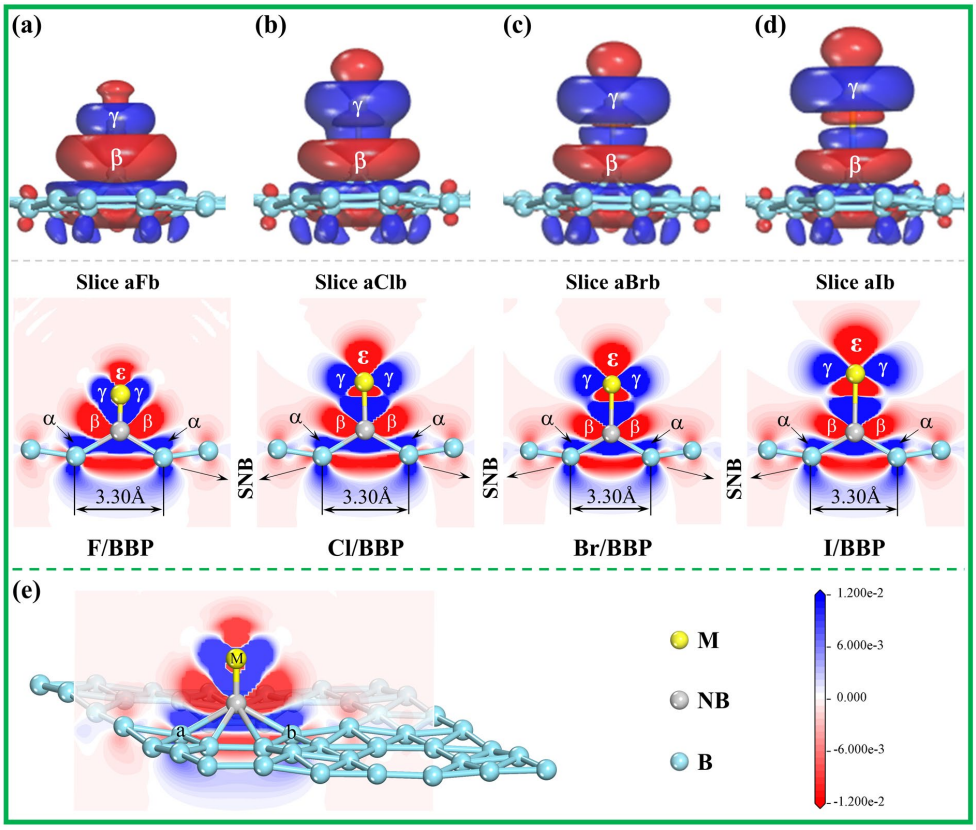

Fig. S20 Electron density differences (Δρ) for (a) F/BBP, (b) Cl/BBP, (c) Br/BBP, (d) I/BBP, and (e) diagram of M and two boron atoms used to determine the indicated slice aMb. SNB represents the sub-neighboring boron of M/BBP. The 3D side-view electron density differences are shown on the surface at an electron density isovalue of 0.008 e/A^3 within the given color scale. The Δρ is defined as Δρ = ρ(M/BBP) – ρ(M) – ρ(BBP), where ρ(M/BBP), ρ(M), and ρ(BBP) represent the electron densities of M/BBP, free M adatoms, and BBP, respectively. The blue and red regions indicate electron accumulation and depletion, respectively. The yellow, gray, and cyan spheres represent adatoms, neighboring borons (NBs) and boron atoms other than NBs (RBs), respectively.

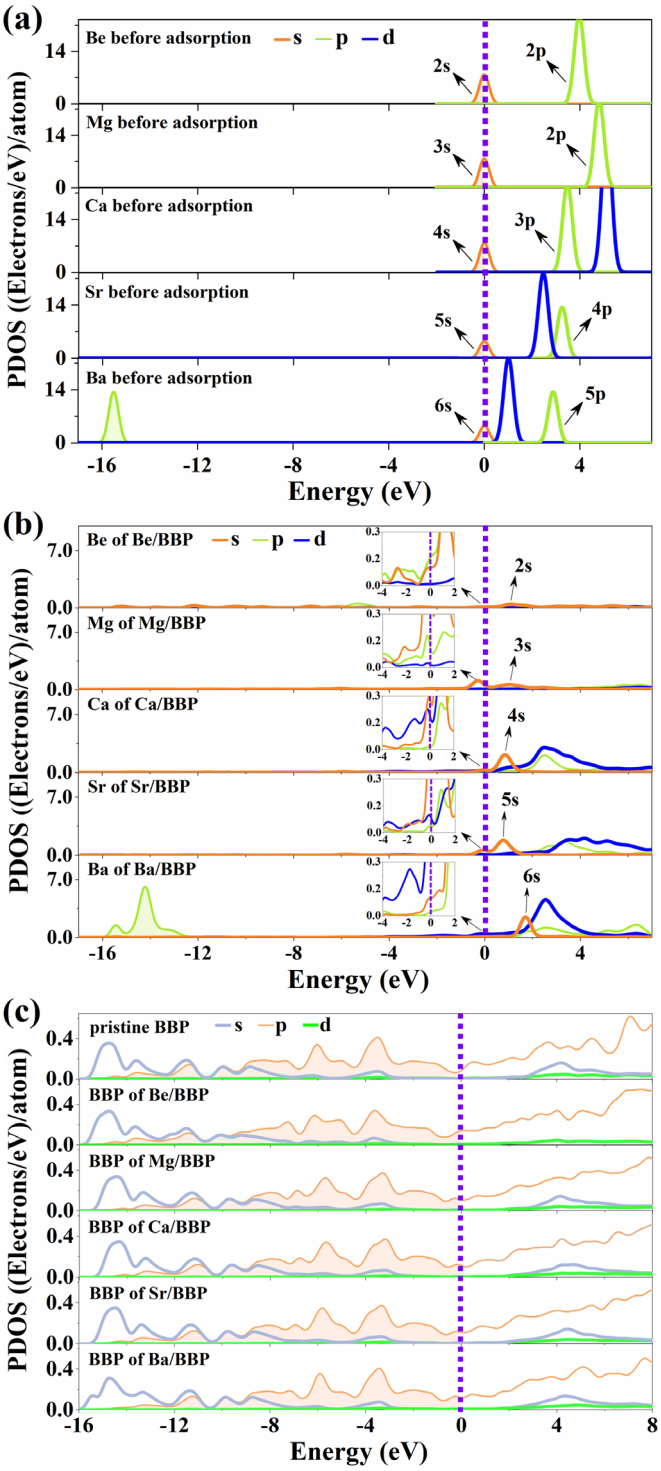

Fig. S21 (a) PDOSs of the s, p, and d orbitals of alkaline earth metal atoms before adsorption. (b) PDOSs of the s, p, and d orbitals of alkaline earth metal atoms after adsorption. (c) PDOSs of the s, p, and d orbitals of boron atoms of alkaline earth metal/BBP before and after adsorption.

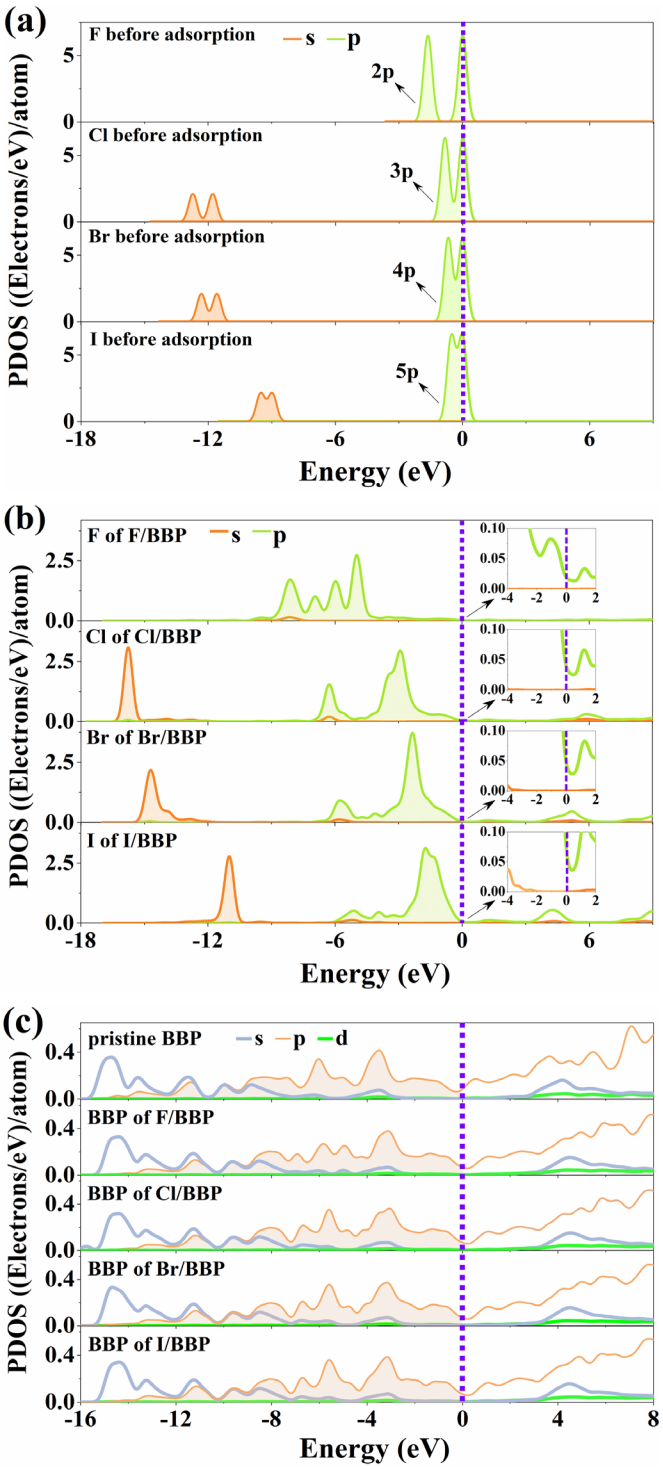

Fig. S22 (a) PDOSs of the s, p, and d orbitals of halogen atoms before adsorption. (b) PDOSs of the s, p and, d orbitals of halogen atoms after adsorption. (c) PDOSs of the s, p, and d orbitals of boron atoms of halogen/BBP before and after adsorption.

References

1. K. T. Chan, J. B. Neaton and M. L. Cohen, *Phys. Rev. B*, 2008, **77**, 235430.
2. M. Legesse, F. E. Mellouhi, E. T. Bentria, M. E. Madjet, T. S. Fisher, S. Kais and F. H. Alharbi, *Appl. Surf. Sci.*, 2017, **394**, 98–107.
3. M. Legesse, S. N. Rashkeev, F. Al-Dirini and F. H. Alharbi, *Appl. Surf. Sci.*, 2020, **509**, 144893.
4. P. D. Taylor, D. A. Osborne, S. A. Tawfik, T. Morishita and M. J. S. Spencer, *Phys. Chem. Chem. Phys.*, 2019, **21**, 7165–7173.
5. J. H. Hao, Z. J. Wang, Y. F. Wang, Y. H. Yin, R. Jiang and Q. H. Jin, *Solid State Sci.*, 2015, **50**, 69–73.
6. B. Zheng, H. T. Yu, Y. Xie and Y. F. Lian, *ACS Appl. Mater. Interfaces*, 2014, **6**, 19690–19701.
7. Y. Y. Deng, Y. Y. Qian, Y. Xie, L. Zhang, B. Zheng, Y. Q. Lou and H. T. Yu, *Acta Chim. Sin.*, 2020, **78**, 344–354.
8. T. Yi, B. Zheng, H. Yu and Y. Xie, *Chem. Res. Chin. Univ.*, 2017, **33**, 631–637.
9. B. Zheng, Y. Xie, Y. Y. Deng, Z. Q. Wang, Y. Q. Lou, Y. Y. Qian, J. He and H. T. Yu, *Adv. Theory Simul.*, 2020, **4**, 1900249.
10. Y. Y. Qian, B. Zheng, Y. Xie, J. He, J. M. Chen, L. Yang, X. Lu and H. T. Yu, *Langmuir*, 2021, **37**, 11027−11040.
11. A. A. Kistanov, Y. Cai, K. Zhou, N. Srikanth, S. V. Dmitriev and Y. W. Zhang, *Nanoscale*, 2018, **10**, 1403–1410.
12. S. S. Li, C. W. Zhang, W. X. Ji, F. Li, P. J. Wang, S. J. Hu, S. S. Yan and Y. S. Liu, *Phys. Chem. Chem. Phys.*, 2014, **16**, 15968–15978.
13. S. D. Sherpa, G. Levitin and D. W. Hess, *Appl. Phys. Lett.*, 2012, **101**, 111602.
14. H. Cho, S. Dae Kim, T. H. Han, I. Song, J. W. Byun, Y. H. Kim, S. Kwon, S. H. Bae, H. Cheul Choi, J. H. Ahn and T. W. Lee, *2D Mater.*, 2014, **2**, 014002.
15. B. Mortazavi, A. Dianat, O. Rahaman, G. Cuniberti and T. Rabczuk, *J. Power Sources*, 2016, **329**, 456–461.
16. C. Ataca, E. Aktürk and S. Ciraci, *Phys. Rev. B*, 2009, **79**, 041406.
17. R. Pekoz, M. Konuk, M. E. Kilic and E. Durgun, *ACS Omega*, 2018, **3**, 1815–1822.